15. Huang SC, Phelps ME, Hoffman EJ, Sideris K, Selin CJ, Kuhl DE. Noninvasive determination of local cerebral metabolic rate of glucose in man. *Am J Physiol* 1980;238:E69–E82.
16. Haberkorn U, Reinhardt M, Strauss LG, et al. Metabolic design of combination therapy: use of enhanced fluorodeoxyglucose uptake caused by chemotherapy. *J Nucl Med* 1992;33:1981–1987.
17. Haberkorn U, Oberdorfer F, Klenner T, et al. Metabolic and transcriptional changes in osteosarcoma cells treated with chemotherapeutic drugs. *Nucl Med Biol* 1994;21:835–845.
18. D'Argenio DZ, Schumitzky A. *ADAPT II User's Guide*. Los Angeles: Biomedical Simulation Resource, University of Southern California; 1992.
19. Sachs L. *Angewandte Statistik*. Berlin: Springer; 1984: 329–333.
20. Higashi K, Clavo AC, Wahl R. In vitro assessment of 2-fluoro-2-deoxy-D-glucose, L-methionine and thymidine as agents to monitor the early response of a human adenocarcinoma cell line to radiotherapy. *J Nucl Med* 1993;34:773–779.
21. Keyes JW. SUV: standardized uptake or silly useless value? *J Nucl Med* 1995;36: 1836–1839.
22. Lacko L, Wittke B, Kromphardt H. Kinetics of glucose uptake in erythrocytes: effect of trans-concentration. *Eur J Biochem* 1972;25:447–454.
23. Haberkorn U, Morr I, Oberdorfer F, et al. Fluorodeoxyglucose uptake in vitro: aspects of method and effects of treatment with gemcitabine. *J Nucl Med* 1994;35:1842–1850.
24. Slosman DO, Pugin J. Lack of correlation between tritiated deoxyglucose, thallium-201 and technetium-99m-MIBI cell incorporation under various cell stresses. *Eur J Nucl Med* 1994;35:120–126.
25. Minn H, Kangas L, Kellokumpu-Lehtinen P, et al. Uptake of 2-fluoro-2-deoxy-D-(U-^{14}C)-glucose during chemotherapy in murine Lewis lung tumor. *Nucl Med Biol* 1992;19:55–63.
26. Hayes N, Biswas C, Strout V, Berger J. Activation by protein synthesis inhibitors of glucose transport into L6 muscle cells. *Biochem Biophys Res Commun* 1993;190:881–887.
27. Shawver LK, Olson SA, White MK, Weber MJ. Degradation and biosynthesis of the glucose transporter protein in chicken embryo fibroblasts transformed by the src oncogene. *Mol Cell Biol* 1987;7:2112–2118.
28. Widnell CC, Baldwin SA, Davies A, Martin S, Pasternak CA. Cellular stress induces a redistribution of the glucose transporter. *FASEB J* 1990;4:1634–1637.
29. Pasternak CA, Aiyathurai JEJ, Makinde V. Regulation of glucose uptake by stressed cells. *J Cell Physiol* 1991;149:324–331.
30. Clancy BM, Czech MP. Hexose transport stimulation and membrane redistribution of glucose transporter isoforms in response to cholera toxin, dibutyryl cyclic AMP and insulin in 3T3 adipocytes. *J Biol Chem* 1990;265:12434–12443.
31. Flier JS, Mueckler MM, Usher P, Lodish HF. Elevated levels of glucose transport and transporter messenger RNA are induced by ras or src oncogenes. *Science* 1987;235: 1492–1495.
32. Hughes CS, Shen JW, Subjeck JR. Resistance to etoposide induced by three glucose-regulated stresses in Chinese hamster ovary cells. *Cancer Res* 1989;49:4452 4454.
33. Wertheimer E, Sasson S, Cerasi E, Ben-Neriah Y. The ubiquitous glucose transporter GLUT-1 belongs to the glucose-regulated protein family of stress-inducible proteins. *Proc Natl Acad Sci USA* 1991;88:2525–2529.
34. Christman D, Crawford EJ, Friedkin M, Wolf AP. Detection of DNA synthesis in intact organisms with positron-emitting (methyl-^{11}C)thymidine. *Proc Natl Acad Sci USA* 1972;69:988–992.
35. Poupeye EM, Goethals PP, Dams RF, De Leenheer AP, van Eijkeren ME. Evaluation of (^{11}C)thymidine for measurement of cell proliferation in fast dividing tissues. *Nucl Med Biol* 1993;20:359–362.
36. Shields AF, Coonrod DV, Quackenbush RC, Crowley JJ. Cellular sources of thymidine nucleotides: studies for PET. *J Nucl Med* 1987;28:1435–1440.
37. Shields AF, Lim K, Grierson J, Link J, Krohn KA. Utilization of labeled thymidine in DNA synthesis: studies for PET. *J Nucl Med* 1990;31:337–342.
38. Vander Borght TM, Lambotte LE, Pauwels SA, Dive CC. Uptake of thymidine labeled on carbon 2: a potential index of liver regeneration by positron emission tomography. *Hepatology* 1990;12:113–118.
39. Shields AF, Grierson JR, Kozawa SM, Zheng M. Development of labeled thymidine analogs for imaging tumor proliferation. *Nucl Med Biol* 1996;23:17–22.

Localization of Iodine-125-mIP-Des-Met^{14}-Bombesin (7-13)NH_2 in Ovarian Carcinoma Induced to Express the Gastrin Releasing Peptide Receptor by Adenoviral Vector-Mediated Gene Transfer

Buck E. Rogers, Maryland E. Rosenfeld, M.B. Khazaeli, Galina Mikheeva, Murray A. Stackhouse, Tiepu Liu, David T. Curiel and Donald J. Buchsbaum

Departments of Radiation Oncology, Medicine, and Gene Therapy Program, Comprehensive Cancer Center, University of Alabama at Birmingham, Birmingham, Alabama

The gastrin releasing peptide receptor (GRPr) has a high affinity for the 14 amino acid bombesin peptide. For this analysis, [^{125}I]-Tyr^4-bombesin was compared with [^{125}I]-mIP-bombesin (a seven amino acid bombesin analog) for in vitro binding and internalization into tumor cells and for tumor localization in vivo. Also, a recombinant adenoviral vector (AdCMVGRPr) was used for gene transfer to induce the expression of GRPr in human ovarian cancer cells for binding and tumor localization with these radiolabeled peptides. **Methods:** [^{125}I]-mIP-bombesin was synthesized and compared with [^{125}I]-Tyr^4-bombesin in internalization assays using BNR-11 cells (mouse fibroblast cells stably transfected with GRPr) over a 24-hr period. In vitro binding assays used BNR-11, and A427, HeLa and SKOV3.ip1 human cancer cells, which were either uninfected or infected with AdCMVGRPr. Biodistribution studies were performed in normal BALB/c mice and in athymic nude mice bearing orthotopic SKOV3.ip1 ovarian cancer tumors. The SKOV3.ip1 tumors were induced to express GRPr with the AdCMVGRPr adenoviral vector. **Results:** Internalization assays showed that [^{125}I]-Tyr^4-bombesin was rapidly internalized and catabolized at 37°C with ≈10% of the radioactivity remaining intracellularly at 4 hr, compared with ≈30% with [^{125}I]-mIP-bombesin. HeLa, A427 and SKOV3.ip1 cells were all induced to express levels of GRPr that were higher than those seen with the positive control BNR-11 cells. Normal mice showed a lower level of radioactivity in both the blood and thyroid for [^{125}I]-mIP-bombesin [0.26% ± 0.10% injected dose per gram (ID/g) and 0.24% ± 0.05% ID] than for [^{125}I]-Tyr^4-bombesin (3.5% ± 1.6% ID/g and 5.2% ± 4.4% ID) at 4 hr postinjection. Mice bearing intraperitoneal (i.p.) SKOV3.ip1 tumors and given AdCMVGRPr i.p. 5 days after tumor cell inoculation followed by [^{125}I]-mIP-bombesin i.p. at day 7 showed 16.5% ± 4.8% ID/g in tumor compared with 5.9% ± 3.0% ID/g with [^{125}I]-Tyr^4-bombesin at 4 hr postinjection. Tumor bearing mice given saline or a control adenovirus expressing the β-galactosidase (LacZ) gene showed significantly lower tumor uptake values of both bombesin peptides. **Conclusion:** Internalization assays showed that [^{125}I]-mIP-bombesin has favorable characteristics compared with [^{125}I]-Tyr^4-bombesin with regards to cellular internalization and retention. The results demonstrate successful in vitro and in vivo transduction of human tumor cells with a recombinant adenoviral vector-expressing GRPr. Additionally, tumors transduced in vivo to express GRPr demonstrated significantly greater localization of [^{125}I]-mIP-bombesin when compared with [^{125}I]-Tyr^4-bombesin.

Key Words: bombesin; gastrin releasing peptide receptor; adenovirus; gene transfer; iodine-125

J Nucl Med 1997; 38:1221–1229

Received Aug. 20, 1996; revision accepted Nov. 13, 1996.

For correspondence or reprints contact: Donald J. Buchsbaum, PhD, Department of Radiation Oncology, University of Alabama at Birmingham, 1824 6th Avenue South, Birmingham, AL 35294.

The use of radiolabeled monoclonal antibodies for tumor diagnosis and therapy (*1,2*) is of great interest; however, there are limitations to the use of these agents (*3*). One approach to addressing low target antigen expression has recently been described in which gene therapy methods were used to increase the expression of antigen on tumor cells (*4–6*). Raben et al. showed that D54 MG human glioma cells could be genetically induced to express the human carcinoembryonic antigen both in vitro and in vivo through the use of a recombinant adenoviral vector and that these cells could subsequently be targeted by radiolabeled COL-1 anti-carcinoembryonic antigen monoclonal antibody (*5*).

Other studies have used gene transfer methods to induce receptors in vitro, which have a high affinity for radiolabeled peptides (*6–8*). In particular, the recombinant adenoviral vector (AdCMVTRHr) was used to induce the expression of the thyrotropin releasing hormone (TRH) receptor in vitro with subsequent binding of [^{3}H]-methyl-TRH (*6–9*). However, this three amino acid peptide cannot be radiolabeled with a variety of therapeutic radionuclides and maintain high receptor affinity. Therefore, a peptide that has a high affinity for its cellular receptor (nanomolar range), which can be labeled with a therapeutic radionuclide without loss of receptor affinity, and that resists in vivo degradation long enough to achieve tumor localization, is required for peptide radiotherapy. In this regard, we chose to investigate bombesin (Fig. 1), a 14 amino acid peptide that has a high affinity for the gastrin releasing peptide receptor (GRPr) (*10*) as the target ligand.

The recombinant adenoviral vector (AdCMVGRPr) was used to induce the expression of the GRPr in vitro in several human carcinoma cell lines and in vivo in a well-established mouse model of human ovarian cancer (*11,12*). This gene was chosen because the GRPr has a high affinity for bombesin and its analogs (*10*), and its endogenous expression is limited to neuroendocrine cells in the pulmonary and gastrointestinal tracts, which would lead to low normal organ uptake of the radiolabeled bombesin peptides. Bombesin has been modified by replacing the leucine in the fourth position with tyrosine (Tyr^4-bombesin) for labeling with iodine (Fig. 1). Thus, Tyr^4-bombesin could be labeled with ^{131}I for therapeutic use. Recently, a bombesin analog, meta-iodophenyl-Des-Met^{14}-bombesin(7-13)NH_2 (mIP-bombesin) (Fig. 1), has been synthesized by Hoffman et al. and shown in a competitive inhibition assay to have an IC_{50} value (the concentration of inhibitor that causes a 50% reduction in radiolabeled bombesin binding) that was almost an order of magnitude lower than bombesin with Swiss 3T3 mouse fibroblast cells (*13,14*). Another study showed that a similar analog can be prepared in which a bifunctional chelate has been attached and radiolabeled with rhodium-105 (*15*). Therefore, bombesin analogs may have advantages over bombesin with respect to receptor binding affinity, ease of labeling with different radionuclides and in vivo stability.

In this study, we describe the synthesis of [^{125}I]-mIP-bombesin and compare its internalization and catabolism with [^{125}I]-Tyr^4-bombesin in a GRPr positive cell line. Additionally, the in vitro induction of GRPr was accomplished with AdCMVGRPr in the murine BNR-11 cells and the human carcinoma cell lines A427, HeLa and SKOV3.ip1, and evaluated by [^{125}I]-Tyr^4-bombesin and [^{125}I]-mIP-bombesin receptor binding. The biodistributions of the two radiolabeled peptides were also compared in vivo in normal mice. Subsequently, the localization of these peptides in mice bearing SKOV3.ip1 ovarian tumors, induced in vivo to express GRPr, was also investigated. Thus, this method of achieving radiolabeled peptide tumor localization through genetic induction of receptors in tumor cells represents a novel approach for peptide imaging or peptide radiotherapy.

MATERIALS AND METHODS

All chemicals were purchased from Aldrich (Milwaukee, WI) unless noted otherwise. Na^{125}I and [^{125}I]-Tyr^4-bombesin [specific activities of each ≈81.4 TBq/mmol (≈2200 Ci/mmol)] were purchased from DuPont/NEN® Research Products (Boston, MA). Reversed-phase high pressure liquid chromatography (RP-HPLC) was performed on a Bio-Rad MAPS Preparative System 100 (Hercules, CA) with a built-in ultraviolet-absorbance detector and a Beckman Model 170 Radioisotope Detector (Fullerton, CA) connected in series. An Alltech Adsorbosphere (C18, 10 μm, 4.6 × 250 mm) column (Deerfield, IL) was used for RP-HPLC separations. Compounds were eluted using a linear gradient of 80% solvent A to 10% solvent A over 40 min (solvent A = H_2O/0.1% trifluoroacetic acid; solvent B = acetonitrile/0.1% trifluoroacetic acid). A Packard Auto Gamma® 5000 Series gamma counter (Chicago, IL) was used for counting ^{125}I samples. Athymic nude female *nu/nu* mice with a BALB/c background, 4–5 wk old, were obtained from the National Cancer Institute Frederick Research Laboratory (Frederick, MD). Cell lines were obtained from the American Type Culture Collection (Rockville, MD) unless noted otherwise. The peptides, mIP-Des-Met^{14}-bombesin(7-13)NH_2 and Des-Met^{14}-bombesin(7-13)NH_2 were synthesized using solid phase peptide synthesis at the University of Alabama, Birmingham, Comprehensive Cancer Center Peptide Synthesis and Analysis Shared Facility.

Synthesis of ^{125}I-mIP-Des-Met^{14}-Bombesin(7-13)NH_2

N-succinimidyl-3-(tri-n-butylstannyl) benzoate (ATE) was synthesized according to the method described by Zalutsky and Narula (*16*) and was characterized by ^{1}H NMR and mass spectrometry. The radiolabeling of ATE with ^{125}I was similar to that described previously (*16*). Briefly, 25 μl (37 MBq, 1 mCi) of Na^{125}I in NaOH was placed in a borosilicate test tube. To this was added 50 μl of a 60 mg/ml solution of acetic acid in $CHCl_3$, followed by 50 μl of a 90 mg/ml solution of t-butylhydroperoxide in $CHCl_3$. Fifty micrograms of ATE (5 mg/ml) was then added to the Na^{125}I solution and the mixture was incubated at room temperature for 1 hr. The reaction mixture was purified by RP-HPLC and the meta-[^{125}I]iodophenyl-N-hydroxysuccinimide ([^{125}I]mIPNHS) product collected and concentrated. The Des-Met^{14}-bombesin(7-13)NH_2 peptide (Gln-Trp-Ala-Val-Gly-His-Leu-NH_2) (300 μg) was dissolved in 60 μl of 0.1 *M* borate buffer (pH 8.5) and added to the [^{125}I]mIPNHS residue and incubated at room temperature for 1 hr. After incubation, the ^{125}I-mIP-Des-Met^{14}-bombesin(7-13)NH_2 ([^{125}I]-mIP-bombesin) was purified by RP-HPLC in 10% overall radiochemical yield. The retention time for [^{125}I]-mIP-bombesin was identical to the retention time observed for the cold compound (21.8 min). The [^{125}I]-mIP-bombesin was concentrated and redissolved in 10% EtOH/0.1% human serum albumin before use in vitro and in vivo.

Cell Lines

The BNR-11 cell line is a derivative of BALB/B1 mouse fibroblast cells, which were stably transfected with murine GRPr (*17*) (provided by J. Battey, National Cancer Institute, Bethesda, MD). The cells were grown in Dulbecco's modified Eagle's medium (DMEM) containing 4.5 g/liter glucose, 2 m*M* glutamine and 300 μg/ml geneticin supplemented with 10% fetal bovine serum (FBS). The HeLa (human cervical epithelial carcinoma) and SKOV3.ip1 (human ovarian adenocarcinoma) cells were maintained in DMEM containing 4.5 g/liter glucose supplemented with 10% FBS. The SKOV3.ip1 cells were obtained from Janet Price (Baylor University, Houston, TX). The A427 cells are a human nonsmall cell lung carcinoma cell line and were maintained in

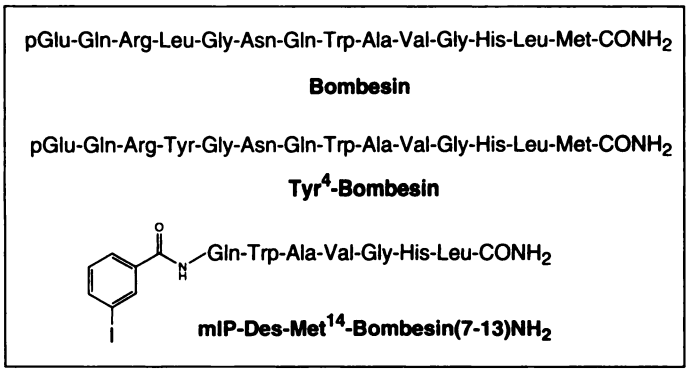

FIGURE 1. Structures of bombesin, Tyr^4-bombesin and mIP-Des-Met^{14}-bombesin(7-13)NH_2.

Eagle's minimum essential medium containing nonessential amino acids and 1 m*M* sodium pyruvate supplemented with 10% FBS.

In Vitro Internalization Assays

The internalization of [^{125}I]-mIP-bombesin and [^{125}I]-Tyr^4-bombesin were compared in vitro with BNR-11 cells using a method similar to that described by Geissler et al. (*18*). The BNR-11 cells were washed with phosphate buffered saline (PBS), detached from flasks by treatment with 4 m*M* EDTA/0.05% KCl, centrifuged and resuspended in serum free media (DMEM containing 4.5 g/liter glucose) at a concentration of 1×10^6 cells/0.5 ml for use in the assay. The cell viability was routinely >85% as determined by trypan blue dye exclusion. The cells were aliquoted (1×10^6) in triplicate into polystyrene test tubes and cooled to 4°C. Either [^{125}I]-Tyr^4-bombesin or [^{125}I]-mIP-bombesin (100 μl; 100,000 cpm) was added to the cells and incubated at 4°C for 1 hr. The cells were centrifuged for 5 min ($500 \times g$; 4°C), the media aspirated and cells resuspended in 1.0 ml of serum free media at 4°C. This was repeated once, the cells were resuspended in 0.5 ml of media containing 2% FBS and placed either on a shaker at 37°C with 5% CO_2 or cooled to 4°C and allowed to incubate for 0, 5, 15, and 30 min, and 1, 2, 4 and 24 hr. At the specified time points, a triplicate of cells was removed from each temperature and centrifuged for 5 min. After centrifugation, the supernatants were removed and saved for counting. The cells were resuspended twice in 0.2 ml of ice-cold 0.2 *M* acetic acid (pH 2.5) and incubated at 4°C for 15 min to remove surface bound activity. The supernatants, acid washes and cells were then counted in a well scintillation gamma counter to determine the amount of internalized, surface bound and supernatant radioactivity.

Construction of a Recombinant Adenoviral Vector Encoding the Human Gastrin Releasing Peptide Receptor cDNA (AdCMVGRPr)

An adenovirus encoding the murine GRPr (mGRPr) cDNA was prepared using standard techniques of in vivo homologous recombination (*19*) and has been described elsewhere (*20*). Briefly, a DNA fragment containing the mGRPr gene was subcloned into the pACCMVpLpARS(+) adenoviral shuttle vector (provided by R. Gerard, Katholieke Universiteit Leuven, Leuven, Belgium). This shuttle plasmid (pAC-mGRPr) and the adenoviral packaging plasmid pJM17 (provided by F. Graham, McMaster University, Hamilton, Ontario, Canada) were cotransfected into the E1A transcomplementing cell line 293 using the commercial cationic liposome vector DOTAP. The newly generated recombinant adenovirus was plaque purified three times and validated by direct polymerase chain reaction. The AdCMVGRPr was titered within the 293 cell line using plaque assay techniques for direct determination of viral plaque forming units (pfu).

In Vitro Infection Using AdCMVGRPr

BNR-11, HeLa, A427 and SKOV3.ip1 cells were grown to >90% confluency in T75 flasks and infected with the AdCMVGRPr adenoviral vector. Briefly, the AdCMVGRPr was added to cells in 4 ml of medium containing 2% fetal calf serum at a multiplicity of infection of 10 or 100 pfu per cell. As a control, cells were also infected with AdCMVLacZ (a control adenovirus that encodes the reporter gene *Escherichia coli* β-galactosidase) (provided by De-Chu Tang, University of Alabama at Birmingham). The cells were incubated for 1 hr at 37°C in 5% CO_2 followed by the addition of 11 ml of complete media. After a 48-hr incubation, the cells were harvested for analysis in a radiolabeled peptide binding assay.

In Vitro Binding of [^{125}I]-Tyr^4-Bombesin and [^{125}I]-mIP-Bombesin in Transduced Cells

Transduced cells (see above) were harvested 48 hr postinfection by rinsing once with PBS followed by an incubation with 4 m*M* EDTA/0.05% KCl for 3 min to detach the cells. Detached cells were rinsed with cold 0.1% BSA/PBS (pH 7.2) and counted, with viability routinely being >85%. The cell suspensions were centrifuged for 5 min at 4°C and the pellets resuspended in cold PBS at a concentration of 2.5×10^6 cells/ml for the binding assay. Each set of cells was aliquoted (100 μl) into polystyrene test tubes in duplicate followed by addition of ≈100,000 cpm (100 μl) of either [^{125}I]-Tyr^4-bombesin or [^{125}I]-mIP-bombesin. The solutions were mixed at room temperature for 1 hr, rinsed with PBE (1% BSA and 0.2 *M* EDTA in 0.1 *M* PBS, pH 7.2) and centrifuged at $1700 \times g$ for 10 min. The supernatant was removed and the cells counted in a gamma counter to determine the amount of bound radioactivity. This was also performed in the presence of at least a 1000-fold molar excess of nonradioactive peptide to determine the nonspecific binding. The results were plotted as the percentage of the counts per minute specifically bound to the cells versus the total counts per minute added.

Biodistribution Studies

Biodistribution experiments were performed in normal BALB/c mice or athymic nude mice implanted intraperitoneally with SKOV3.ip1 cells. The normal mice were administered ≈74 kBq (2 μCi) of either [^{125}I]-Tyr^4-bombesin or [^{125}I]-mIP-bombesin by an intraperitoneal (i.p.) injection, and the animals were killed at 15 and 30 min, and 1, 4 and 12 hr postinjection. The blood, heart, lungs, liver, stomach, small intestine, spleen, kidney, skin, bone, muscle and thyroid were removed, weighed and the activity counted in a gamma counter. The percent injected dose per gram (%ID/g) for each tissue was calculated except for the thyroid, in which only the percent injected dose (%ID) was determined.

For the mouse orthotopic tumor model, 2×10^7 SKOV3.ip1 cells were implanted by means of an i.p. injection and allowed to grow for 5 days. AdCMVGRPr (1×10^9 pfu), AdCMVLacZ (1×10^9 pfu) or saline was then administered by means of an i.p. injection followed 2 days later by an i.p. injection of either [^{125}I]-Tyr^4-bombesin or [^{125}I]-mIP-bombesin. The animals were killed 4 hr postinjection of the radiolabeled peptide, and the tumor and normal organs mentioned above were removed, weighed and counted in a gamma counter.

Statistical Analysis

Descriptive statistics were calculated to examine the distribution and variation of time concentration of radiolabeled peptides (means and s.d.) (*21*). Means were calculated from multiple mice data for both tissue concentration and tumor-to-blood ratios. Mean concentration data (%ID/g) over time in normal mice were used for pharmacokinetic modeling. The pharmacokinetic parameters were estimated by using the nonlinear regression (NLIN) procedure of Statistical Analysis System programs (*22*). An intravenous bolus

administration approach was used to model the time concentration data and to estimate the elimination rate constants. Functions consisting of the sum of one or two exponential components were fit to data by a least squares method. Selection of models was based on comparison of Akaike's Information Criterion and the standard errors of estimates (*22*). It was shown that a one-compartment model best fit the [^{125}I]-Tyr^4-bombesin data, whereas a two-compartment model best fit the [^{125}I]-mIP-bombesin data. Elimination ($t_{1/2}$) values were calculated as well as the area under the curve and mean residence time (*22*).

RESULTS

Synthesis of [^{125}I]-mIP-Bombesin

The synthesis schema of [^{125}I]-mIP-bombesin is shown in Figure 2. The [^{125}I]-mIP-bombesin product was isolated as a single peak in 10% overall radiochemical yield with a radiochemical purity of >95%. The RP-HPLC system fully separated [^{125}I]-mIP-bombesin (21.8 min) from unlabeled Des-Met-bombesin (7-13)NH_2 (13.9 min) and from unreacted [^{125}I]mIPNHS (17.5 min) and its hydrolysis product (14.4 min). A specific activity of greater than 44.4 TBq/mmol (1200 Ci/mmol) was calculated for [^{125}I]-mIP-bombesin on the basis of the ultraviolet detection limit of the HPLC system.

In Vitro Internalization Assays

The rate of internalization of [^{125}I]-mIP-bombesin was compared with [^{125}I]-Tyr^4-bombesin in vitro using BNR-11 cells that stably express GRPr. After 1 hr of incubation at 4°C (time 0), both compounds showed ≈80% of the radioactivity bound to the cell surface, whereas the remaining 20% was retained intracellularly (Fig. 3). Radioactivity bound to the cell surface was rapidly internalized at 37°C for [^{125}I]-Tyr^4-bombesin with only 21.8% ± 0.5% remaining surface bound at 1 hr, whereas [^{125}I]-mIP-bombesin had 48.8% ± 7.9% of the radioactivity surface bound at 1 hr. Cells that were incubated at 4°C showed a constant amount of cell surface, internalized and supernatant radioactivity over the course of the experiment (data not shown). At 37°C, the intracellular radioactivity for [^{125}I]-Tyr^4-bombesin reached a maximum of 41.4% ± 1.3% at 5 min and then rapidly decreased to 14.3% ± 8.4% at 30 min, with only 9.0% ± 2.7% remaining at 4 hr. In contrast, the intracellular radioactivity for [^{125}I]-mIP-bombesin reached a maximum of 37.3% ± 10.9% after 5 min at 37°C but only decreased to 32.0% ± 9.0% by 4 hr. Radioactivity in the supernatant appeared immediately for both compounds; however, by 1 hr, 67.0% ± 5.8% of the radioactivity was in the supernatant for [^{125}I]-Tyr^4-bombesin, whereas only 13.1% ± 1.6% was in the supernatant for [^{125}I]-mIP-bombesin at this time point.

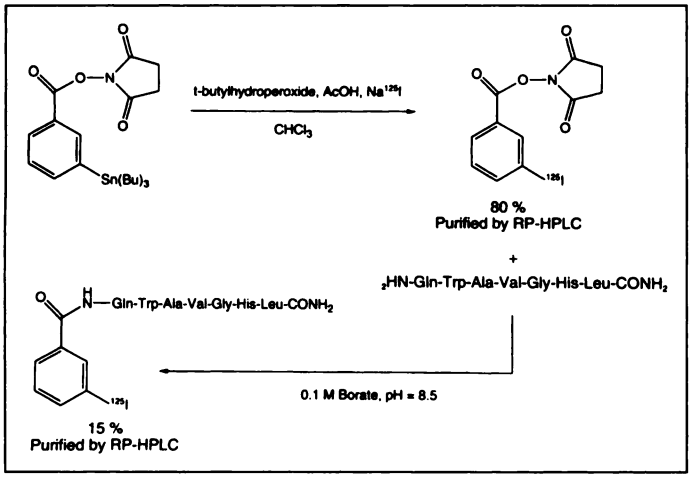

FIGURE 2. Schema for the synthesis of [^{125}I]-mIP-Des-Met^{14}-bombesin (7-13)NH_2.

Binding of [^{125}I]-Tyr^4-Bombesin and [^{125}I]-mIP-Bombesin after In Vitro AdCMVGRPr Infection

BNR-11, A427 and HeLa cells were infected with 10 pfu per cell of AdCMVGRPr to induce expression of GRPr, whereas SKOV3.ip1 cells were infected with 100 pfu per cell. All cell lines were also infected with 100 pfu per cell of AdCMVLacZ as a negative control virus. Expression of GRPr was assessed at 2 days postinfection using [^{125}I]-Tyr^4-bombesin and [^{125}I]-mIP-bombesin in a receptor binding assay. Uninfected murine BNR-11 cells were used as a positive control and showed 25.6% ± 1.6% binding of [^{125}I]-Tyr^4-bombesin and 38.3% ± 11.6% binding of [^{125}I]-mIP-bombesin in two assays run in duplicate (Fig. 4). BNR-11 cells infected with either AdCMVGRPr or AdCMVLacZ showed binding similar to noninfected cells for both radiolabeled ligands. In contrast, when the human carcinoma cells A427, SKOV3.ip1 and HeLa were infected with AdCMVGRPr, all showed levels of [^{125}I]-Tyr^4-bombesin and [^{125}I]-mIP-bombesin binding (60%–88%) that were significantly greater ($p < 0.001$) than BNR-11 cells. Human carci-

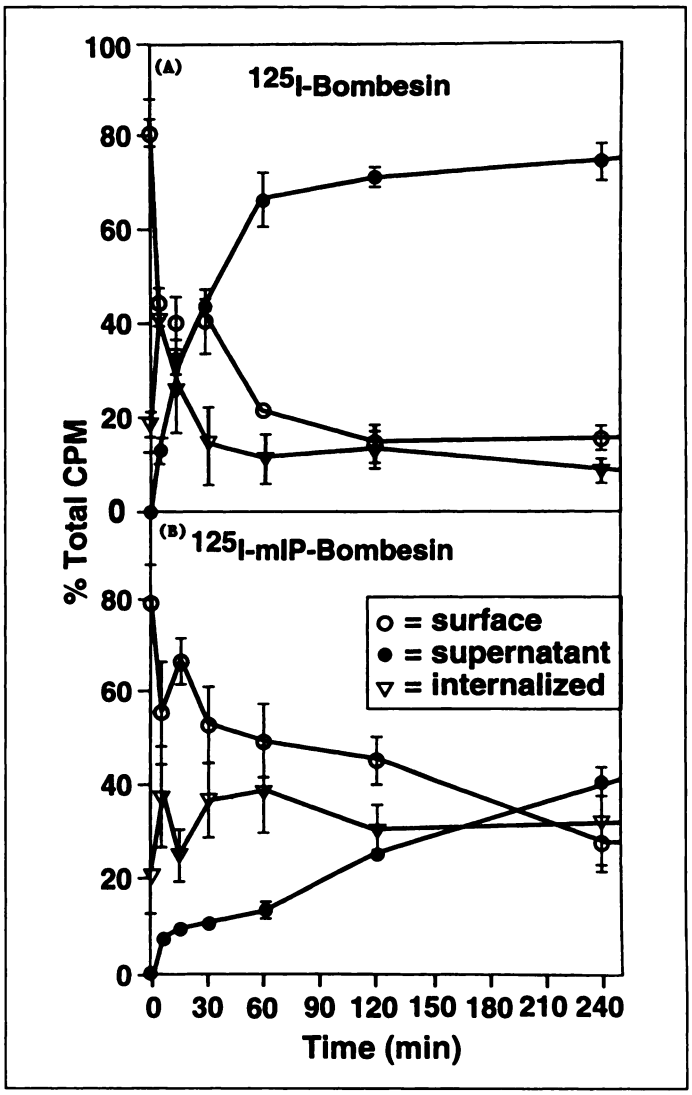

FIGURE 3. Rates of internalization and catabolism of [^{125}I]-Tyr^4-bombesin (A) and [^{125}I]-mIP-bombesin (B) in BNR-11 cells stably transduced to express GRPr. The relative percentage of radioactivity on the cell surface (acid wash, ○), in the supernatant (●) and internalized (cell pellet, ▽), are plotted as a function of time. Each time point represents the mean of triplicate measurements ± s.d.

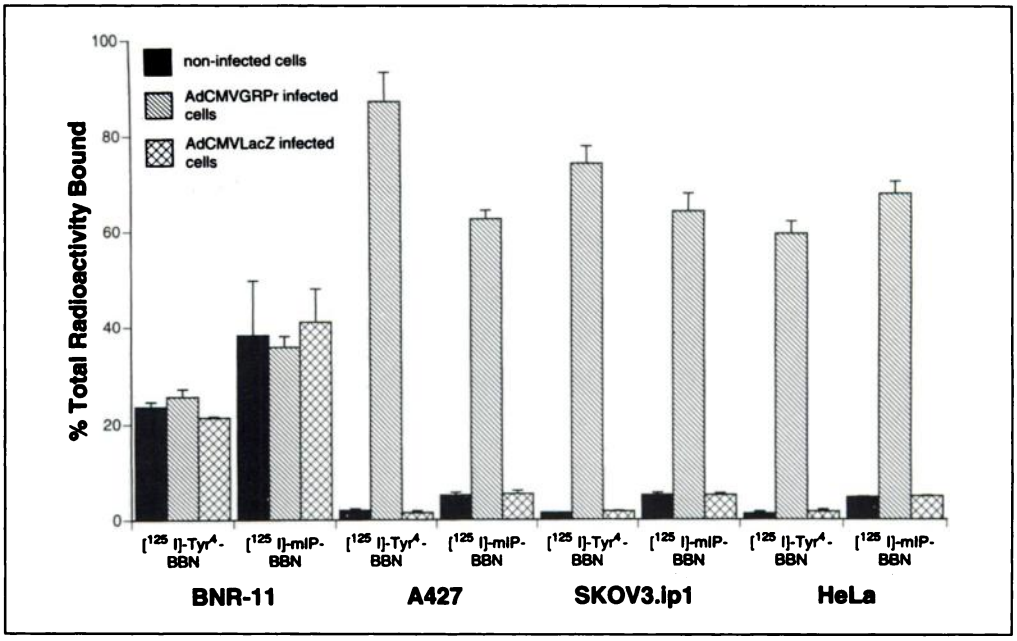

FIGURE 4. Analysis of binding of [^{125}I]-Tyr^4-bombesin ([^{125}I]-Tyr^4-BBN) and [^{125}I]-mIP-bombesin ([^{125}I]-mIP-BBN) to BNR-11, A427, SKOV3.ip1 and HeLa cells, which were either noninfected, infected with AdCMVGRPr or infected with AdCMVLacZ. The bars illustrate the percentage of total radioactivity bound and represent the mean of duplicate or triplicate measurements ± s.d.

noma cells infected with AdCMVLacZ demonstrated a level of radiolabeled ligand binding comparable to noninfected cells (1%–6%).

Biodistribution Studies

The pharmacokinetic parameters and representative curves for the biodistribution of [^{125}I]-Tyr^4-bombesin administered i.p. in normal mice are shown in Table 1 and Figure 5, respectively. The results are presented for a one-compartment model. The highest concentration of [^{125}I]-Tyr^4-bombesin in blood was 6.5% ± 0.3% ID/g at 1 hr postinjection which declined to 0.1% ± 0.01% ID/g at 12 hr postinjection. The clearance half-life ($t_{1/2}$) from blood of [^{125}I]-Tyr^4-bombesin was 2.2 hr, whereas the other tissues ranged from 2.0–2.8 hr.

The pharmacokinetic parameters and representative curves for the [^{125}I]-mIP-bombesin administered i.p. to normal mice are shown in Table 2 and Figure 6, respectively. The results are presented for a two-compartment model. The highest concentration of [^{125}I]-mIP-bombesin in the blood was 3.0% ± 1.7% ID/g at 15 min after injection, which declined to 0.1% ± 0.02% ID/g at 12 hr after injection. The initial clearance half-life ($t_{1/2\alpha}$) from blood of [^{125}I]-mIP-bombesin was 0.1 hr, whereas its secondary half-life ($t_{1/2\beta}$) was 7.6 hr. The $t_{1/2\alpha}$ for [^{125}I]-mIP-bombesin from other tissues was 0.1 hr and the $t_{1/2\beta}$ ranged from 2.3 to 25.4 hr.

The differences in rate of deiodination of the two compounds can be observed by the accumulation of radioactivity in the thyroid and stomach (Fig. 7). The thyroid uptake for [^{125}I]-Tyr^4-bombesin 1 hr after injection was 4.8% ± 0.8% ID compared with 0.2% ± 0.1% ID for [^{125}I]-mIP-bombesin ($p < 0.001$). Similarly, the stomach uptake for [^{125}I]-Tyr^4-bombesin 1 hr postinjection was significantly greater than the uptake of [^{125}I]-mIP-bombesin (16.2% ± 3.6% ID versus 1.1% ± 0.4% ID, respectively; $p < 0.001$).

Biodistributions of the radiolabeled ligands were also determined in athymic nude mice bearing intraperitoneal SKOV3.ip1 tumors that were induced to express GRPr with AdCMVGRPr. The biodistributions of [^{125}I]-Tyr^4-bombesin and [^{125}I]-mIP-bombesin in tumor bearing mice that were administered saline or AdCMVLacZ were similar to that in normal mice. Figure 8 shows the biodistributions of both radiolabeled ligands in tumor bearing mice that were treated with AdCMVGRPr and AdCMVLacZ (saline data not shown, but similar to AdCMVLacZ results). The tumor uptake of [^{125}I]-mIP-bombesin (16.5% ± 4.8% ID/g) in mice administered AdCMVGRPr was significantly greater than the uptake of [^{125}I]-Tyr^4-bombesin (5.9% ± 3.0% ID/g; $p = 0.006$). These tumor values are also significantly greater than values obtained from mice that were administered AdCMVLacZ ([^{125}I]-mIP-bombesin = 0.5% ± 0.1% ID/g; $p < 0.001$; [^{125}I]-Tyr^4-bombesin = 2.1% ± 1.0% ID/g; $p = 0.007$). The tumor-to-blood ratios of [^{125}I]-Tyr^4-bombesin and [^{125}I]-mIP-bombesin in AdCMVLacZ- and AdCMVGRPr-treated mice at 4 hr postinjection are shown in Figure 9. [^{125}I]-Tyr^4-bombesin had a tumor-to-blood ratio of 0.6 ± 0.1 in mice that were given AdCMVLacZ compared with 1.4 ± 0.5 in mice treated with AdCMVGRPr ($p = 0.005$). The difference in tumor-to-blood ratio between mice administered AdCMVLacZ or AdCMVGRPr was greatly enhanced when the [^{125}I]-mIP-bombesin analog was used (2.3 ± 0.7 versus 74.5 ± 24.3, respectively) ($p < 0.001$). The induction of GRPr in other abdominal organs such as the liver, small intestine, spleen, uterus and the lining of the abdominal cavity by AdCMVGRPr can also be observed by the uptake of [^{125}I]-Tyr^4-bombesin or [^{125}I]-mIP-bombesin when compared with AdCMVLacZ treated mice. However, SKOV3.ip1 cells are known to form malignant ascites and nodules around organs within the peritoneum (*12*).

DISCUSSION

Our goal in these studies was to develop a new approach to radioimmunotherapy by targeting radiolabeled peptides towards tumors that have been genetically induced to express receptors with a high affinity for these radiolabeled ligands. We constructed a recombinant adenoviral vector encoding murine GRPr driven by the CMV promoter to accomplish the expression of GRPr on tumor cells, which can subsequently bind radiolabeled bombesin or bombesin analogs. The use of a xenogeneic receptor/ligand combination such as murine GRPr/bombesin obviates the concern of binding by the endogenous human GRP to the xenogeneic receptor. The radiolabeled bombesin could bind to human GRPr on normal tissues such as the small intestine, which is radiosensitive; however, the level of human GRPr is relatively low on normal tissues.

The bombesin analog, mIP-bombesin, was synthesized by Hoffman et al. and shown to have an IC_{50} value that was almost

TABLE 1
Pharmacokinetic Parameters for Biodistribution of [^{125}I]-Tyr^4-Bombesin in Normal Mice

	C_{max} (%ID/g)	$t_{1/2}$ (hr)	AUC (%ID × hr/g)	MRT (hr)
Blood	6.5	2.2	25.1	3.2
Bone	2.8	2.7	12.8	3.9
Heart	2.5	2.7	11.0	3.8
Kidney	5.4	2.0	19.0	3.0
Liver	3.4	2.4	10.4	3.5
Lung	4.8	2.3	21.2	3.3
Muscle	1.5	2.8	6.8	4.0
Small intestine	8.4	2.1	25.8	3.0
Spleen	5.8	2.3	17.2	3.3

TABLE 2
Pharmacokinetic Parameters for Biodistribution of [^{125}I]-mIP-Bombesin in Normal Mice

	C_{max} (%ID/g)	$t_{1/2\alpha}$ (hr)	$t_{1/2\beta}$ (hr)	AUC (%ID × hr/g)	MRT (hr)
Blood	3.0	0.1	8.0	6.5	7.6
Bone	4.4	0.1	11.1	2.7	12.4
Heart	1.7	0.1	14.9	5.5	16.4
Kidney	20.8	0.1	7.3	18.9	2.6
Liver	8.3	0.1	6.0	15.7	5.8
Lung	2.2	0.1	5.8	11.6	2.3
Muscle	0.7	0.1	13.4	2.1	14.9
Small intestine	46.0	0.1	2.3	56.2	1.1
Spleen	4.9	0.1	25.4	12.1	22.6

an order of magnitude lower than bombesin with 3T3 mouse fibroblast cells (*13,14*). Therefore, we radiolabeled this analog with ^{125}I and compared it to the commercially available [^{125}I]-Tyr^4-bombesin both in vitro and in vivo (*23*). The [^{125}I]mIPNHS was synthesized using a method similar to that described by Zalutsky and Narula (*16*). We synthesized [^{125}I]mIPNHS in ≈80% yield, which is comparable to that described by Zalutsky and Narula. However, when they used this reagent to radiolabel antibodies they achieved yields of about 60% compared with the 10% we achieved when labeling bombesin(7-13). This is likely due to the high number of coupling sites that are available on antibodies compared with the lone amino terminus that was used when coupling with bombesin(7-13).

The internalization of [^{125}I]-Tyr^4-bombesin and [^{125}I]-mIP-bombesin was compared in vitro using BNR-11 cells that were modified to stably express GRPr (*17*). At 37°C, the amount of internalized radioactivity for both compounds reached a maximum of ≈40% at 5 min. This is comparable to other studies that have shown rapid internalization of [^{125}I]-Tyr^4-bombesin in other cell lines (*24*). However, the internalized radioactivity rapidly decreased to 14.3% ± 8.4% at 30 min for [^{125}I]-Tyr^4-bombesin, while only decreasing to 32.0% ± 9.0% at 4 hr for [^{125}I]-mIP-bombesin (Fig. 3). This is likely due to differences in

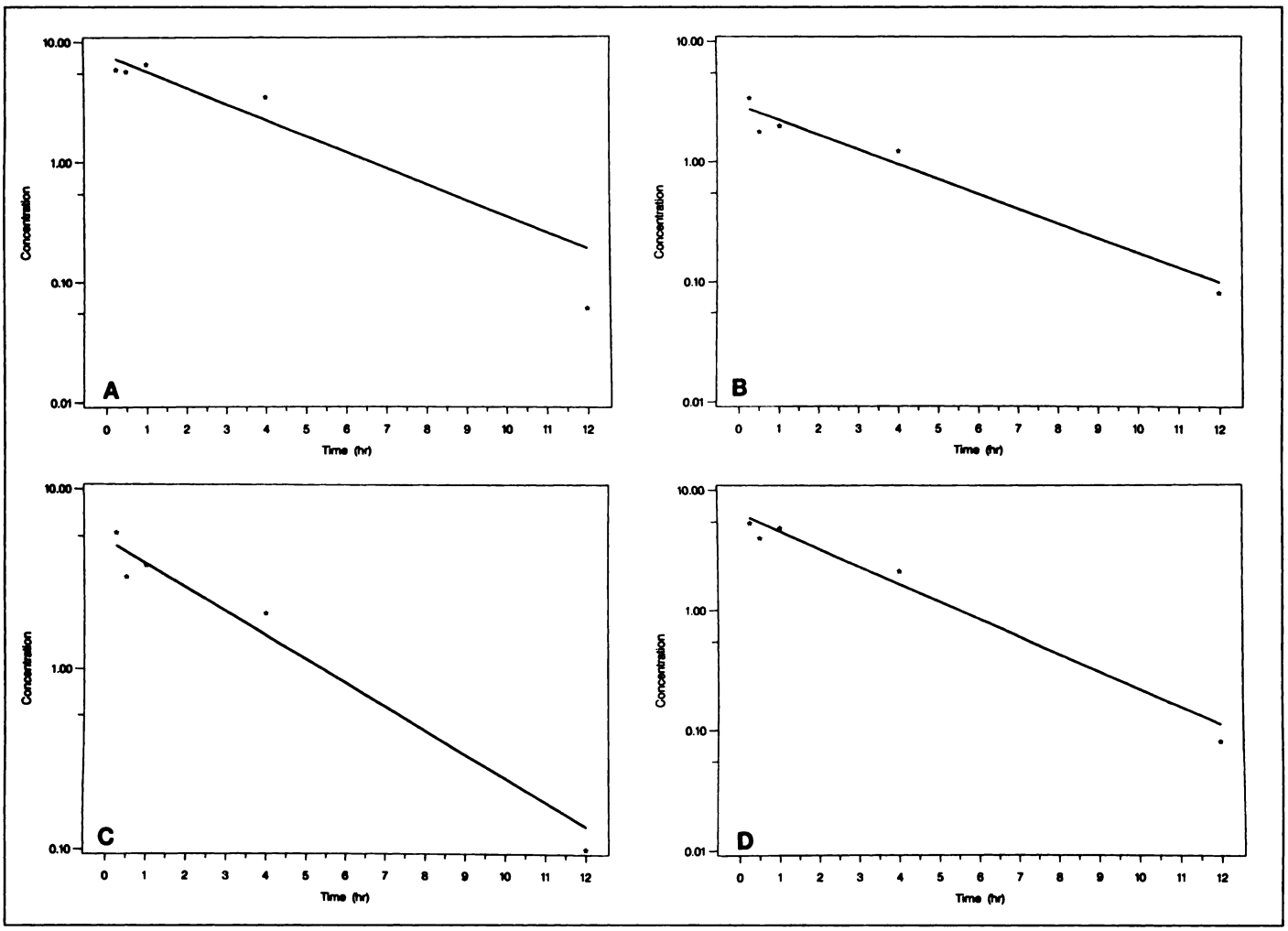

FIGURE 5. Concentration (%ID/g) of [^{125}I]-Tyr^4-bombesin in (A) blood, (B) liver, (C) spleen and (D) kidney at various times after injection. Normal BALB/c mice were injected i.p. with [^{125}I]-Tyr^4-bombesin and killed at 4 hr postinjection.

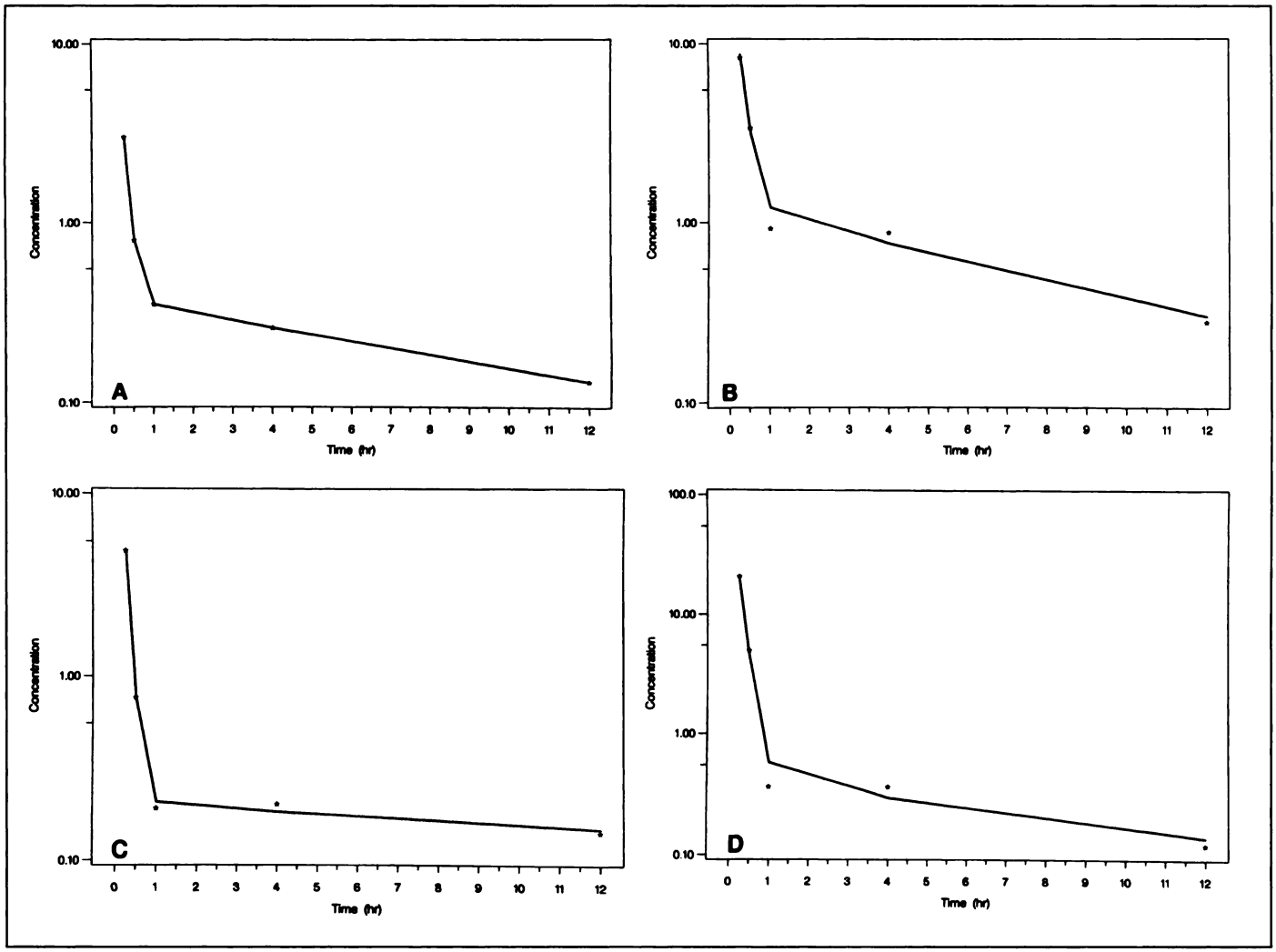

FIGURE 6. Concentration (%ID/g) of [^{125}I]-mIP-bombesin in (A) blood, (B) liver, (C) spleen and (D) kidney at various times after injection. Normal BALB/c mice were injected i.p. with [^{125}I]-mIP-bombesin and killed at 4 hr postinjection.

the rates of cellular release of the catabolic products of the two compounds. Previous studies have shown that proteins are degraded to their individual amino acid components and that proteins labeled with mIPNHS through available ε-amine groups of lysine are degraded to lysine-mIPNHS (*25*). Therefore, it is likely that [^{125}I]-Tyr^4-bombesin was catabolized to [^{125}I]-monoiodotyrosine, and [^{125}I]-mIP-bombesin was catabolized to [^{125}I]-mIP-glutamine [glutamine was the N-terminal amino acid in bombesin(7-13)]. The [^{125}I]-monoiodotyrosine product has an active transport mechanism for cellular release (*18,26*), whereas it is unlikely that the same is true for [^{125}I]-mIP-glutamine.

A recombinant adenoviral vector (AdCMVGRPr) constructed to encode the murine GRPr gene driven by the CMV promoter was evaluated in vitro through the binding of [^{125}I]-Tyr^4-bombesin or [^{125}I]-mIP-bombesin. The human carcinoma cell lines A427, SKOV3.ip1 and HeLa were induced to express GRPr as evidenced by the binding of [^{125}I]-Tyr^4-bombesin and [^{125}I]-mIP-bombesin at 2 days postinfection (Fig. 4). The specificity of this binding is illustrated by the lack of peptide binding when the cells were infected with the control virus, AdCMVLacZ. The positive control BNR-11 cells did not show any enhanced peptide binding when infected with AdCMVGRPr.

Before applying this gene transfer methodology in vivo, the biodistributions of [^{125}I]-Tyr^4-bombesin and [^{125}I]-mIP-bombesin were evaluated in normal BALB/c mice. The clearance of radioactivity from normal tissues after i.p. injection of [^{125}I]-Tyr^4-bombesin and [^{125}I]-mIP-bombesin was rapid. The [^{125}I]-mIP-bombesin showed an early rapid distribution phase and a slower elimination phase, whereas [^{125}I]-Tyr^4-bombesin cleared blood and other tissues with a first order elimination rate. The lower levels of radioiodine in the thyroid and stomach after administration of [^{125}I]-mIP-bombesin suggest that this peptide undergoes less deiodination than [^{125}I]-Tyr^4-bombesin (Fig. 7). This agrees with previous studies that show that radiolabeling of proteins with [^{125}I]mIPNHS resulted in less deiodination than proteins labeled through tyrosine residues (*16,25,27*).

The localization of these peptides was then compared in a regional model of ovarian cancer with athymic nude mice at 7 days after i.p. inoculation of SKOV3.ip1 tumor cells. This tumor model was chosen because human ovarian cancer is primarily confined within the peritoneal cavity, and previous studies have shown that i.p injection of radiolabeled monoclonal antibodies result in higher tumor uptake than intravenous administration (*28,29*). Tumor localization of the ^{125}I-labeled peptides was analyzed 4 hr postinjection, and [^{125}I]-mIP-bombesin demonstrated significantly greater localization compared with [^{125}I]-Tyr^4-bombesin (Fig. 8). This might be expected based on the internalization studies discussed earlier. These differences in tumor localization of the two peptides may also be explained by differences in the extent of deiodination of

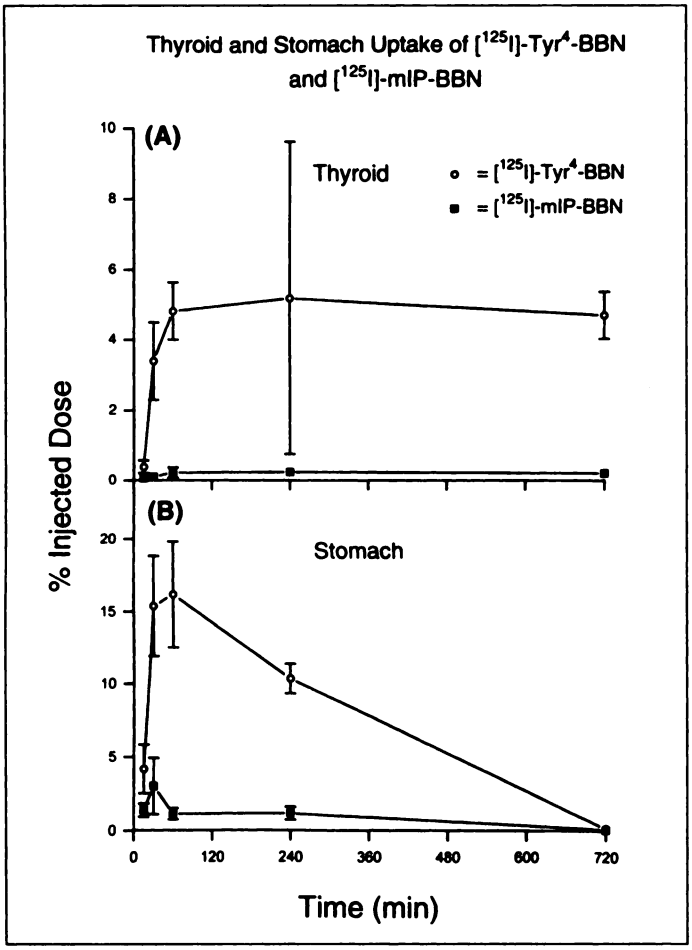

FIGURE 7. Uptake of [^{125}I]-Tyr^4-bombesin ([^{125}I]-Tyr^4-BBN, (○) and [^{125}I]-mIP-bombesin ([^{125}I]-mIP-BBN, ■) in the thyroid and stomach of normal BALB/c mice. Data are expressed as the percent injected dose versus time. Each data point represents the mean of five animals ± s.d.

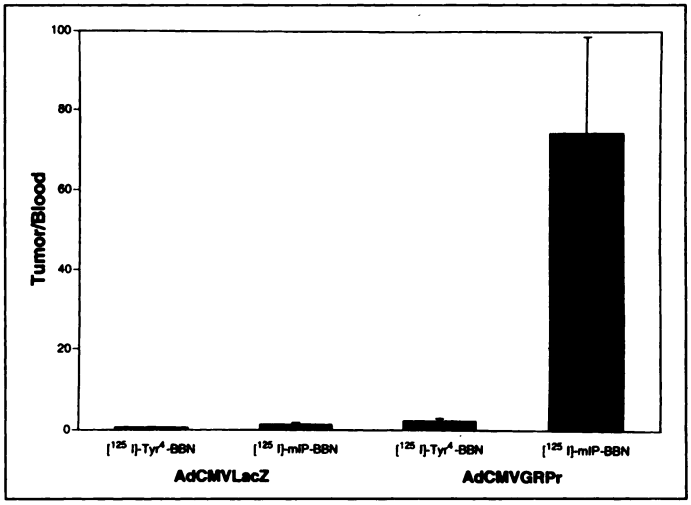

FIGURE 9. Tumor-to-blood ratios of [^{125}I]-Tyr^4-bombesin ([^{125}I]-Tyr^4-BBN) and [^{125}I]-mIP-bombesin ([^{125}I]-mIP-BBN) in athymic nude mice. Mice were inoculated i.p. with 2×10^7 SKOV3.ip1 tumor cells. At day 5, they were injected i.p. with 1×10^9 pfu of either AdCMVGRPr or AdCMVLacZ. Two days after viral administration, animals were injected i.p. with either [^{125}I]-Tyr^4-BBN or [^{125}I]-mIP-BBN and killed 4 hr later. Each data point represents the mean of five animals ± s.d.

the two compounds. When mice were administered either saline or AdCMVLacZ, there was little tumor localization of either peptide, which demonstrated the specificity of GRPr induction. The blood clearance of [^{125}I]-Tyr^4-bombesin and [^{125}I]-mIP-bombesin in this tumor model was similar to that observed in normal mice resulting in a large tumor-to-blood ratio for [^{125}I]-mIP-bombesin. There was also a larger uptake of both compounds in other abdominal organs in mice administered AdCMVGRPr compared with mice given either saline or AdCMVLacZ. This could be due to dissemination of the SKOV3.ip1 tumors to these organs (*12*). Additionally, ectopic expression of GRPr in these organs after AdCMVGRPr delivery is possible and has been reported by others (*30,31*).

One could envision targeting the vector to human tumors in vivo without infecting normal cells in the context of local/regional disease. Adenoviral vectors have been injected into tumor nodules or compartmentally in animals with high vector concentrations and containment (*32,33*). For disseminated disease, transductional (*34*) or transcriptional techniques (*35–37*) have been developed that could be used to restrict expression to tumors. This component of the targeting issue will be the subject of future work.

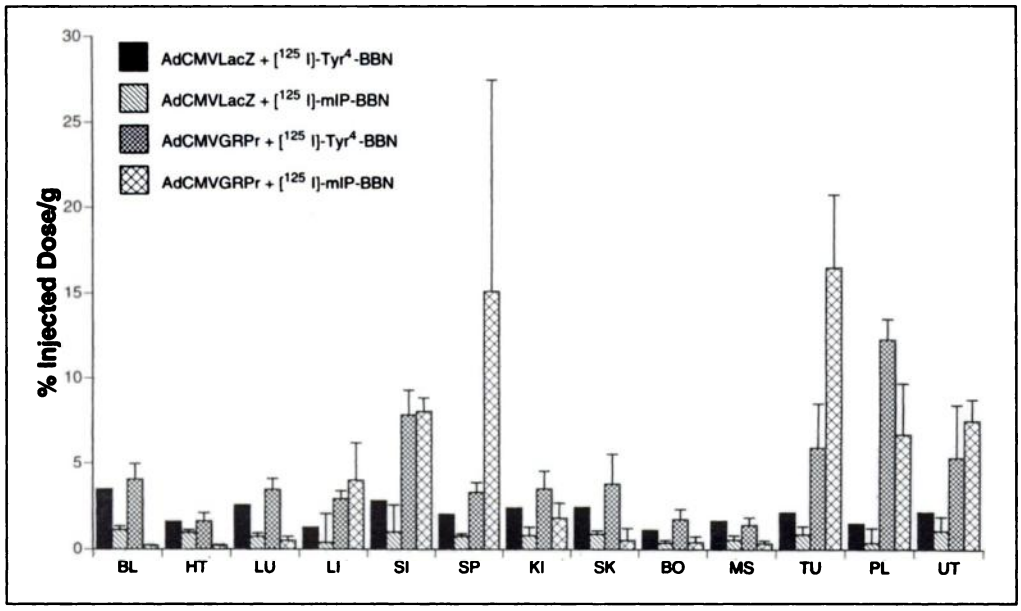

FIGURE 8. Biodistribution of bombesin analogs in athymic nude mice. Mice were inoculated i.p. with 2×10^7 SKOV3.ip1 tumor cells. At day 5, they were injected i.p. with 1×10^9 pfu of the appropriate adenovirus. Two days after viral administration, animals were injected i.p. with the radiolabeled ligands and killed 4 hr later. BL = blood; HT = heart; LU = lung; LI = liver; SI = small intestine; SP = spleen; KI = kidney; SK = skin; BO = bone; MS = muscle; TU = tumor; PL = lining of abdominal cavity; UT = uterus. Each bar represents the mean of five animals ± s.d.

CONCLUSION

The aim of this study was to demonstrate that a novel approach for tumor diagnosis or therapy, which combines the use of radiolabeled peptides with the genetic induction of high affinity receptors on tumors, is rational. We described the synthesis of [^{125}I]-mIP-bombesin and showed that it had more favorable internalization properties than [^{125}I]-Tyr^4-bombesin in a live-cell binding assay and that it had better tumor localization in an ovarian tumor model induced to express the GRPr with an adenoviral vector. This localization may be enhanced even further through the use of an adenovirus containing a tissue-specific promoter. Future studies will investigate the therapeutic efficacy of radiolabeled bombesin analogs in mice bearing tumors induced to express GRPr.

ACKNOWLEDGMENTS

We would like to thank Richard Kirkman, Sheila Bright, Casey Jones, Terra Ragland, Kim Laffoon and Stephanie McLean for their excellent technical assistance. Thanks also go to Sally Lagan for help in the preparation of this manuscript. This work was supported by Department of Energy Grant DE-FG05–93ER61654 (D.J.B.). Portions of this work were previously presented at the Society of Nuclear Medicine 43rd Annual Meeting in Denver, CO, 1996.

REFERENCES

1. Goldenberg DM. New developments in monoclonal antibodies for cancer detection and therapy. *CA-Cancer J Clin* 1994;44:43–64.
2. Jurcic JG, Scheinberg DA. Radioimmunotherapy of hematological cancer: problems and progress. *Clin Cancer Res* 1995;1:1439–1446.
3. Buchsbaum DJ. Experimental radioimmunotherapy and methods to increase therapeutic efficacy. In: Goldenberg, D. M., ed. *Cancer therapy with radiolabeled antibodies.* Boca Raton, FL: CRC Press; 1995:115–140.
4. Hand PH, Robbins PF, Salgaller ML, Poole DJ, Schlom J. Evaluation of human carcinoembryonic-antigen (CEA)-transduced and non-transduced murine tumors as potential targets for anti-CEA therapies. *Cancer Immunol Immunother* 1993;36:65–75.
5. Raben D, Buchsbaum DJ, Khazaeli MB, et al. Enhancement of radiolabeled antibody binding and tumor localization through adenoviral transduction of the human carcinoembryonic antigen gene. *Gene Ther* 1996;3:567–580.
6. Buchsbaum DJ, Raben D, Stackhouse MA, et al. Approaches to enhance cancer radiotherapy employing gene transfer methods. *Gene Ther* 1996;3:1042–1068.
7. Falck-Pedersen E, Heinflink M, Alvira M, Nussenzveig DR, Gershengorn MC. Expression of thyrotropin-releasing hormone receptors by adenovirus-mediated gene transfer reveals that thyrotropin-releasing hormone desensitization is cell specific. *Mol Pharmacol* 1994;45:684–689.
8. Hinuma S, Hosoya M, Ogi K, et al. Molecular cloning and functional expression of a human thyrotropin-releasing hormone (TRH) receptor gene. *Biochim Biophys Acta* 1994;1219:251–259.
9. Raben D, Buchsbaum DJ, Khazaeli MB, et al. Strategies to augment radioimmunotherapy via genetic induction of receptors for radioligand binding. *Cancer Gene Ther* 1995;2:330.
10. Moody TW, Cuttitta F. Growth factor and peptide receptors in small cell lung cancer. *Life Sci* 1993;52:1161–1173.
11. Yu D, Wolf JK, Scanlon M, Price JE, Hung MC. Enhanced c-erbB-2/neu expression in human ovarian cancer cells correlates with more severe malignancy that can be suppressed by E1A. *Cancer Res* 1993;53:891–898.
12. Deshane J, Siegal GP, Alvarez RD, et al. Targeted tumor killing via an intracellular antibody against erbB-2. *J Clin Invest* 1995;96:2980–2989.
13. Hoffman TJ, Sieckman GL, Volkert WA. Targeting small cell lung cancer using iodinated peptide analogs. *J Labeled Compd Radiopharm* 1995;37:321–323.
14. Hoffman TJ, Sieckman GL, Volkert WA. Iodinated bombesin analogs: effect of N-terminal versus side chain iodine attachment on BBN/GRP receptor binding. *J Nucl Med* 1996;37:185P.
15. Ning L, Hoffman TJ, Sieckman GL, et al. In vitro and in vivo characterization of a Rh-105-tetrathiamacrocycle conjugate of a bombesin analog. *J Nucl Med* 1996;37:61P.
16. Zalutsky MR, Narula AS. A method for the radiohalogenation of proteins resulting in decreased thyroid uptake of radioiodine. *Appl Radiat Isot* 1987;38:1051–1055.
17. Battey JF, Way JM, Corjay MH, et al. Molecular cloning of the bombesin/gastrin-releasing peptide receptor from Swiss 3T3 cells. *Proc Natl Acad Sci USA* 1991;88:395–399.
18. Geissler F, Anderson SK, Venkatesan P, Press O. Intracellular catabolism of radiolabeled anti-μ antibodies by malignant B-cells. *Cancer Res* 1992;52:2907–2915.
19. Becker TC, Noel RJ, Coats WS, et al. Use of recombinant adenovirus for metabolic engineering of mammalian cells. *Methods Cell Biol* 1994;43:161–189.
20. Rosenfeld ME, Rogers BE, Khazaeli MB, et al. Adenoviral mediated delivery of gastrin releasing peptide receptor results in specific tumor localization of a bombesin analog in vivo. *Clin Cancer Res* 1997;3:1187–1194.
21. Snedecor GW, Cochran WG. *Statistical methods*, 7th ed. Ames, IA: The Iowa State University Press; 1980.
22. Liu T. Characteristics of pharmacokinetics modeling in a phase I clinical trial of radiolabeled monoclonal antibody. *Controlled Clin Trials* 1991;12:654–655.
23. Rogers BE, Stackhouse M, Khazaeli MB, et al. Evaluation of a radioiodinated bombesin analog as a potential radiotherapeutic agent. *J Nucl Med* 1996;37:186P.
24. Zhu WY, Goke B, Williams JA. Binding, internalization and processing of bombesin by rat pancreatic acini. *Am J Physiol* 1991;261:G57–G64.
25. Garg PK, Alston KL, Welsh PC, Zalutsky MR. Enhanced binding and inertness to dehalogenation of α-melanotropic peptides labeled using N-succinimidyl 3-iodobenzoate. *Bioconjugate Chem* 1996;7:233–239.
26. Press OW, Shan D, Howell-Clark J, et al. Comparative metabolism and retention of iodine-125, yttrium-90 and indium-111 radioimmunoconjugates by cancer cells. *Cancer Res* 1996;56:2123–2129.
27. Zalutsky MR, Noska MA, Colapinto EV, Garg PK, Bigner DD. Enhanced tumor localization and in vivo stability of a monoclonal antibody radioiodinated using N-succinimidyl 3-(tri-n-butylstannyl)benzoate. *Cancer Res* 1989;49:5543–5549.
28. Rowlinson G, Snook D, Busza A, Epenetos AA. Antibody-guided localization of intraperitoneal tumors following intraperitoneal or intravenous antibody administration. *Cancer Res* 1987;47:6528–6531.
29. Ward BG, Mather SJ, Hawkins LR, et al. Localization of radioiodine conjugated to the monoclonal antibody HMFG2 in human ovarian carcinoma: assessment of intravenous and intraperitoneal routes of administration. *Cancer Res* 1987;47:4719–4723.
30. Brody SL, Jaffe A, Han SK, Wersto RP, Crystal RG. Direct in vivo gene transfer and expression in malignant cells using adenovirus vectors. *Hum Gene Ther* 1994;5:437–447.
31. Smythe WR, Kaiser LR, Hwang HC, et al. Successful adenovirus-mediated gene transfer in an in vivo model of human malignant mesothelioma. *Ann Thorac Surg* 1994;57:1395–1401.
32. Wills KN, Maneval DC, Menzel P, et al. Development and characterization of recombinant adenoviruses encoding human p53 for gene therapy of cancer. *Hum Gene Ther* 1994;5:1079–1088.
33. Cusack JC, Spitz FR, Nguyen D, et al. High levels of gene transduction in human lung tumors following intralesional injection of recombinant adenovirus. *Cancer Gene Ther* 1996;3:245–249.
34. Douglas JT, Rogers BE, Rosenfeld ME, et al. Targeted gene delivery by tropism-modified adenoviral vectors. *Nat Biotechnol* 1996;14:1574–1578.
35. Garver RI, Jr, Goldsmith KT, Rodu B, et al. Strategy for achieving selective killing of carcinomas. *Gene Ther* 1994;1:46–50.
36. Smith MJ, Rousculp MD, Goldsmith KT, Curiel DT, Garver RI Jr. Surfactant protein A-directed toxin gene kills lung cancer cells in vitro. *Hum Gene Ther* 1994;5:29–35.
37. Tanaka T, Kanai F, Okabe S, et al. Adenovirus-mediated prodrug gene therapy for carcinoembryonic antigen-producing human gastric carcinoma cells in vitro. *Cancer Res* 1996;56:1341–1345.